Analysis of Test D1.1 of the LIFUS5/Mod3 facility for In-box LOCA in WCLL-BB

Samad Khani Moghanaki[a]*, Francesco Galleni[a], Marica Eboli[b], Alessandro Del Nevo[b], Sandro Paci[a], Nicola Forgione[a]

[a]*DICI – University of Pisa, Largo L. Lazzarino 2, 56122 Pisa, Italy*
[b]*ENEA FSN-ING-SIS, CR Brasimone, 40032 Camugnano (BO), Italy*

**Corresponding author: s.khanimoghanaki@studenti.unipi.it*

Abstract

The in-box Loss of Coolant Accident (LOCA) scenario is considered as one of the most affecting safety concerns for the Water-Cooled Lithium Lead Breeding Blanket (WCLL-BB) modules of the DEMOnstration (DEMO) reactor, which is sequentially followed by a multi-phase multi-component physical and chemical interaction. Therefore, the transient behavior of such accidents has to be carefully investigated during the design phase of the plant, to evaluate the consequences and to adopt the necessary mitigating countermeasures. This also requires a numerical predictive tool, which is capable to model such transients and predict the relevant phenomena under an operational condition and the connected safety parameters i.e. system pressure, temperature, chemical products mass, and volume fractions of all the existing components. Consequently, the SIMMER-III code was firstly improved at the University of Pisa by implementing the chemical reaction between PbLi eutectic alloy and water. In addition to this, an experimental campaign and a test-matrix has been recently designed according to the LIFUS5/Mod3 facility to perform a series of experiments and code post-test analyses.

In the present work, the experimental data of the first LIFUS5/Mod3 test is used for the validation of the chemical model implemented in SIMMER-III through a comprehensive sensitivity study. The applied methodology for the code validation is based on a three-step procedure including qualitative analysis, quantitative analysis and the results from sensitivity analyses. The qualitative accuracy evaluation is performed through a systematic comparison between experimental and calculated time trends based on the engineering analysis, the resulting sequence of main events and the identification of phenomenological windows and of relevant thermo-hydraulic aspects. Afterwards, the accuracy of the code prediction is evaluated from a quantitative point of view by means of selected, widely used, figures of merit. Finally, the results from the sensitivity cases are analyzed and quantified, to determine the effects of the most influencing code input options and transient parameters.

Furthermore, the analysis is followed by applying the Fast Fourier Transform Method (FFTM) to the experimental signals and all the sensitivity calculations. The comparison shows a very good agreement for pressure transient between the experimental and numerical data, while for the temperature and the hydrogen production the results fall into acceptable criteria, which means that the code is reliable in capturing and predicting the transient values but not perfectly match with the experimental signals.

Keywords: WCLL-BB, DEMO reactor, in-box LOCA, SIMMER-III, Code assessment, Fast Fourier Transform Method

1. Introduction

The Breeding Blanket (BB) system is one of the main safety components of the DEMO reactor, which is currently under design and will be built as the prototype machine for the first generation of commercial thermonuclear fusion power plants. Considering the whole BB system, it plays three important roles: firstly, to interface the plasma and remove the heat and transfer it to the Primary Heat Transfer System (PHTS); secondly, to regenerate (breed) the tritium consumed in the fusion reaction in order to ensure the tritium self-sufficiency; thirdly, to provide a thermal and nuclear radiation shielding. Since BB is the first contacting medium, which indirectly interacts with the plasma surface, the features of the blanket system can highly affect the safety performance of the DEMO reactor [1]. Water-Cooled Lithium-Lead (WCLL BB) is considered among the four alternative options (which is newly shortened to two promising options as HCPB and WCLL) for the European DEMO nuclear fusion reactor [2], [3], which will be tested during ITER operation through the Test Blanket Module (TBM) program [4].

The in-box LOCA accident, (ref. [5]), is the most relevant safety concern for the BB systems and, for a WCLL breeding blanket, it is defined as an injection of pressurized water (155 bar and 295-328°C, the same pressure and temperature as the primary loop of a PWR reactor) into the liquid PbLi phase, which exists at 330°C and rather low pressure (1 bar). This accident is followed by a thermodynamic-chemical interaction between PbLi as the breeding medium and water as the coolant. This transient contributes to the pressurization of the PbLi loop while an hydrogen gas generation occurs at the same time [6]. Comprehensive studies could be found in the literature, aimed to address the safety response of the WCLL BB system in case of a postulated in-box LOCA, see [6] and [7]. For this purpose, an advanced R&D activity was started, under the EUROfusion consortium agreement, by a bilateral collaboration between the Experimental Engineering Division of ENEA Brasimone and the Nuclear Thermohydraulic Research Group of the University of Pisa. The activity consists in the numerical simulation, based on SIMMER-III code, of a set of experimental tests on LIFUS5/Mod3 test facility.

The facility was previously constructed and newly upgraded to fulfill the requirements of such experimental activity at ENEA [7]. The results from the experimental campaigns have been employed for the SIMMER-III code validation purpose. These campaigns will also contribute to providing a useful database for the future Verification and Validation of a new System Thermal Hydraulic 2D (STH/2D) coupling calculation tool [8], [9] under development at the University of Pisa.
The present work aims to interpret the results of the first test of the Series D experimental campaign, so called Test D1.1, which was performed on LIFUS5/Mod3 facility [10]. A standard validation method, including quantitative and qualitative analyses, has been considered to elaborate the numerical data against the experimental results, based on a three-step evaluation process [11], previously applied for Separate Effect Test (SET) code validation purpose ref. [12]. Verification and Validation procedures were established and conducted by using the modified version of SIMMER-III for fusion applications, to obtain a qualified numerical tool for deterministic safety analysis. The verification activity was successfully completed (ref. [13]) and documented within the past numeric-analytical and experimental activities (ref. [13]), while the validation phase requires further efforts according with the R&D plan set up in the framework of the EUROfusion Project, ref. [6]. This approach consists of qualitative, quantitative and sensitivity analyses.

2. Experimental campaign on LIFUS5/Mod3 facility

2.1. Facility description

LIFUS5/Mod3 is a separate effect test facility that consists of modifying the existing LIFUS5/Mod2 test facility (see refs. [14]and [15] for more details) with a new smaller reaction vessel (S1B). The “section B” of the facility applies the S1B vessel and will be used in the framework of EUROfusion program, to investigate the PbLi-water interaction, Fig. 1. The main objectives of the present work can be explained as the investigation of the relevant physical and chemical phenomena between lead-lithium eutectic alloy and water, and the validation of the chemical model of the SIMMER-III code. Additionally, the expected outcomes of the experiments are listed below:

- The generation of a detailed and reliable experimental database;
- The improvement of the knowledge of thermodynamic and chemical behaviour of the PbLi eutectic alloy;
- The investigation of the dynamic effects of energy release on the structures, which is out of the scope of this paper, and of the chemical reaction and hydrogen production.

The LIFUS5/Mod3-section B is fully described in ref. [16] and the main components are listed in Tab. 1.

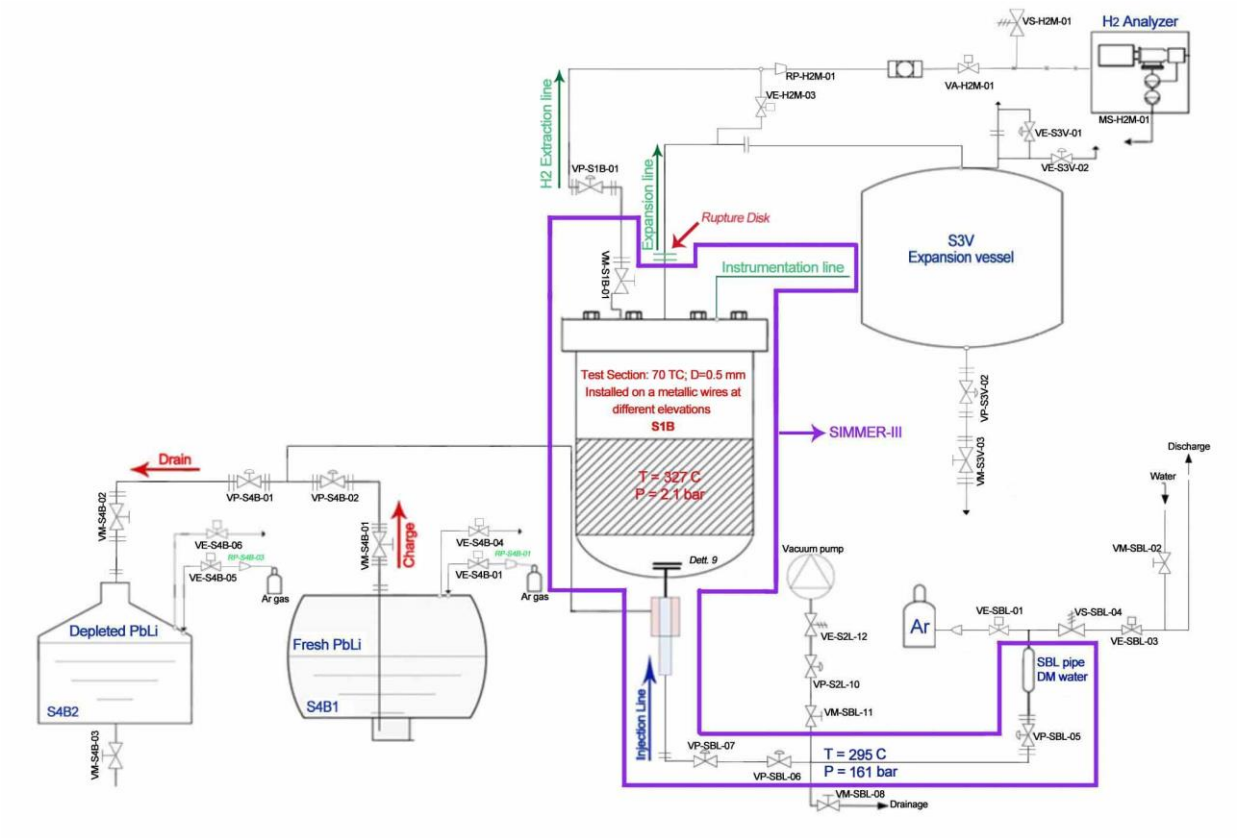

Fig. 1: LIFUS5/Mod3 configuration, to be used for the SIMMER-III reference model

Component	Parameter	Value
S1-B Reaction vessel	Volume [m^3]	0.03
	Inner diameter [m]	0.257
	Height [m]	0.556
	Operating pressure [bar]	>160
	Operating temperature [°C]	480
S2 Water pipe	Volume [m^3]	0.004
	Inner diameter [m]	0.043
	Design pressure [bar]	200
	Design temperature [°C]	350
S3 Dump vessel	Volume [m^3]	2.0
	Inner diameter [m]	1
	Design pressure [bar]	10
	Design temperature [°C]	400
S4-B1 Fresh PbLi	Volume [m^3]	0.40
	Diameter of cylindrical part [m]	0.544
	Length [m]	1.56+ends
	Operating temperature [°C]	400
S4-B2 Depleted PbLi	Volume [m^3]	0.40
	Diameter of cylindrical part [m]	0.544
	Length [m]	1.56+ends
	Operating temperature [°C]	400

Tab. 1: LIFUS5/Mod3: vessels main dimensions and operating features

2.2. Procedure of Test D1.1

The experimental campaign on LIFUS5/Mod3 consists of two test series, so-called Series D and Series E. In the tests of Series D, only a specific amount of water is charged and injected into the reaction vessel (S1B) through the injection line. The first test of this kind, named Test D1.1, was performed with 50 g of water at 295°C and 161 bar. The test procedure can be subdivided into 3 sequential steps:

PbLi charging: The PbLi charging phase started by heating up the lead-lithium charging line and the reaction vessel S1B to 300°C, and the alloy in the storage tank S4B1 to 340°C. This temperature difference allows thermocouples to sense the passage of the liquid metal. Argon gas was passed through all components, to remove any remaining air that would interact with the alloy. Once the line was ready for charging, Argon gas was inserted into S4B1 vessel through the valve VE-S4B-01, see Fig. 1. The pressure exerted by the gas on the alloy pushed it into the loading line and inside the reaction vessel. During this phase, thermocouples installed at different levels on the top of Test Section sense the alloy level, which shall be between the top of the test section's perforated plate and the upper flange of S1B. Based on the acquired signals from the relevant Thermo-Couples (TCs), it turned out that the PbLi level covers the first level and did not reach the second level, above the perforated plate of test section. When the alloy was in position, VP-S4B-02 was closed and the overpressure extracted from S4B1. The temperatures (set points on the heating system) were set to the test conditions and the thermal insulation removed from the loading line, to freeze the alloy and isolate the storage tanks from the reaction vessel.

Test Execution: The initial test conditions were achieved accordingly with the design specifications, a detailed explanation of experimental procedure, the test matrix for Series D and the main parameters characterizing the tests are reported in [10]. The water injection is started by opening the valve VP-SBL-06 and ended by its closure, which was automatically activated after 1 s, therefore, the injection into S1B lasted 1.1 s (from the injector cap rupture to VP-SBL-06 fully closed). The amount of water injected in S1B was pre-defined as 50 g. The Test D1.1 transient was divided in 3 main phases:

- Phase 1: Injection line pressurization, recorded by PT-SBL-02;
- Phase 2a: Coolant flashing and reaction vessel pressurization, from the injection cap rupture up to the onset of the first pressure peak in the S1B reaction vessel;
- Phase 2b: Pressurization due to the water and gas injections and to the hydrogen generation;
- Phase 2c: Characterized by the continuous gas injection, up to the pressure stabilization;
- Phase 3: System stabilization, from the valve closing signal up to the end of transient.

Hydrogen Extraction: At the end of the injection procedure, the hydrogen gas extraction line (VP-S1B-01) was opened, without waiting for the lead-lithium to freeze. The hydrogen analysis proceeded by pushing the produced hydrogen toward the hydrogen analyzer unit, by means of pressurized argon gas. The majority of the gas phase (including hydrogen) has been analysed within the reliable range of the flow meter, resulting in a total of 3.07 ± 0.18 g of hydrogen at 4 hours 45 minutes from the beginning of the analysis. This result is in the range foreseen and calculated by the stoichiometry. Indeed, for 50 g of injected water, the hydrogen produced by the reaction shall be in the range between 2.7 and 5.5 g, according to the predominant reaction between PbLi and water.

3. SIMMER-III model

3.1. Geometrical domain and reference nodalization

The facility set up for the reference model calculation is shown in Fig. 1. The following 5 main parts were considered for the nodalization:

- The injection line (including all the valves, the SBL pressurized water pipe and the injector cap);
- The reaction vessel S1B (including the Test-Section);
- The expansion line (including the first rupture disk);
- Hydrogen extraction line (up to the collecting valve);
- Thermocouple supporting passage (gooseneck).

Based on the LIFUS5/Mod3 facility configuration, a new model was developed through SIMMER-III to support the experimental campaign as reference model. Since SIMMER-III uses cylindrical coordinates, it is possible to reproduce only axial-symmetric domains and, therefore, it is important to notice that the developed nodalization actually used a cylindrical geometry to model the reaction vessel S1B, injection line and the connecting parts. The reaction vessel S1B, the injection line, the supporting passage for the thermocouples, the hydrogen extraction line, the expansion line, are all included in this model as halved symmetric volumes.

The geometrical domain is obtained by 50 radial and 100 axial mesh cells. The SIMMER-III nodalization is shown in Fig. 2, in which each color distinguishes the different fluids and structure materials, as set at the beginning of the transient (i.e., $t = 0\ s$). In particular, with reference to Fig. 2, the PbLi is represented in red, the water in blue, the argon cover gas (and the hydrogen produced by the reaction) in white, the non-calculation zones are highlighted by green mesh fence and

SS316 in black as the structural material. The reference mesh cells for the temperature analysis inside the S1B, representing the position of installed TCs on Test Section of S1B, are highlighted in yellow (see Fig. 2) and listed in Tab. 2. The test Section of S1B consists of 6 rings and 6 levels, which is supported by a welded steel structure and placed inside the S1B vessel. Each ring from this Test Section supports three TCs, which are radially fixed on the ring with an equal 120° orientation and named with respect to the number of its ring and level. For instance, the TC-R13-L2 represents the third installed TC on the first ring and in the second level of the Test Section. A schematic view of Test Section is shown in Fig. 3. The reference cells for the pressure measuring are also highlighted in purple (see Fig. 2) and listed in Tab. 2.

The numerical simulation has been performed by "SIMMER-III Ver. 3F", which is the code version modified at the University of Pisa for fusion applications [13], implementing the model for the PbLi/Water chemical reaction.
The main SIMMER-III code options for the reference calculation are described in refs. [17] and [18], and summarized hereafter:

- Inter-cell heat transfer applied between all the liquid components and solid particles, in vapor, in the structures, and between structures and liquid components;
- Adjustment of vapor temperature in the two-phase cells having a very small void fraction to avoid instabilities in numerical calculations;
- The chemical reaction model applied to take account of the Lithium (in the form of PbLi alloy) and water reaction in both liquid and vapor forms.

The orifice coefficients of enlargement/constriction and curves, implemented in the input file, are calculated by means of empirical correlations [19]. The acquired data from the experiment (Test D1.1) were employed at the relevant cells as Boundary and Initial Conditions (BIC) for the post-test simulation, see Tab. 3. The acquired data from PC-SBL-01 and TC-SBL-01 were applied at cell (19,50) as boundary condition values for the argon gas pressure and temperature, respectively. The test matrix information is described in ref. [7].

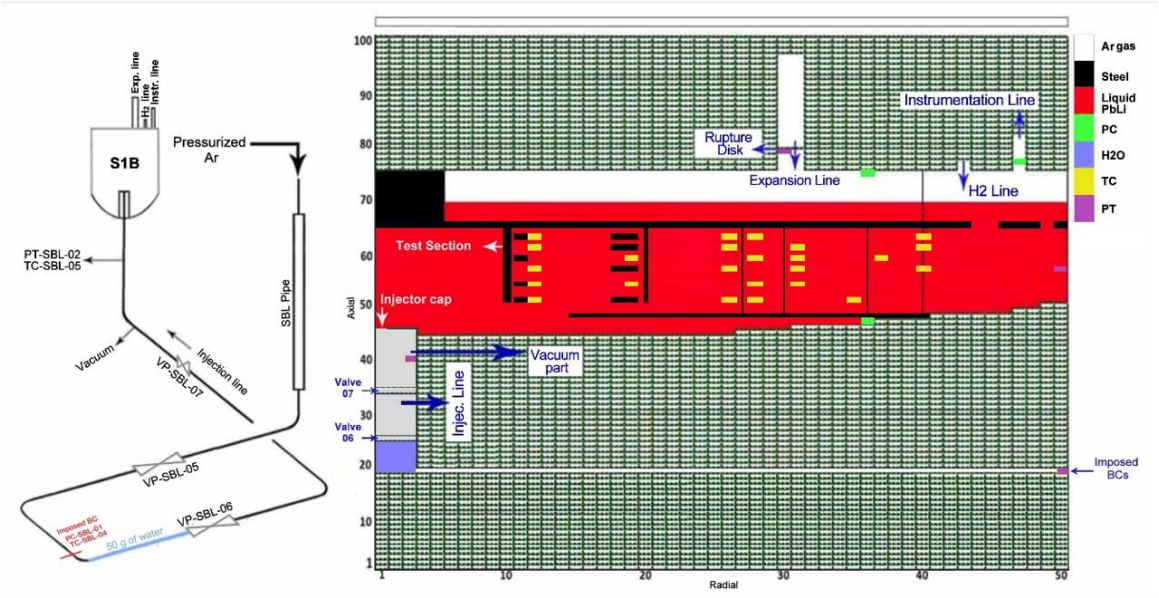

Fig. 2: Reference nodalization for the SIMMER III model

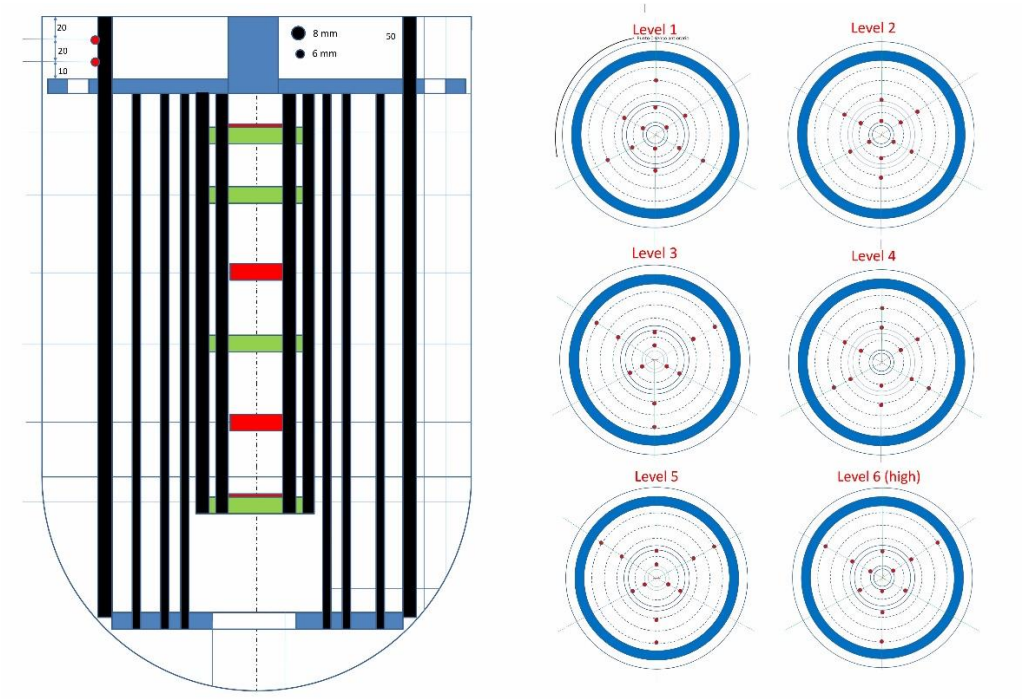

Fig. 3: Test Section; the position of installed TCs in S1B

Installed (TCs), in the Test Section							
	Ring 1	**Ring 2**	**Ring 3**		**Ring 4**	**Ring 5**	**Ring 6**
Level 1	(12,51)	-	(26,51)	(28,51)	-	(35,51)	-
	TC-R11-L1/ TC-R13-L1		TC-R31-L1/ TC-R32-L1/ TC-R33-L1	TC-R34-L1/ TC-R35-L1/ TC-R36-L1		TC-R53-L1	
Level 2	(12,54)	(19,54)	(28,54)		(31,54)	-	-
	TC-R11-L2/ TC-R12-L2/ TC-R13-L2	TC-R21-L2/ TC-R22-L2	TC-R32-L2/ TC-R33-L2		TC-R41-L2/ TC-R42-L2/ TC-R43-L2		
Level 3	(12,57)	-	(26,57)		(31,57)	-	(41,57)
	TC-R12-L3/ TC-R13-L3		TC-R31-L3/ TC-R33-L3		TC-R41-L3/ TC-R42-L3/ TC-R43-L3		TC-R61-L3/TC-R62-L3/ TC-R63-L3
Level 4	-	(19,59)	(28,59)		(31,59)	(37,59)	-
		TC-R21-L4/ TC-R22-L4/ TC-R23-L4	TC-R31-L4/ TC-R32-L4/ TC-R33-L4		TC-R41-L4/ TC-R42-L4/ TC-R43-L4	TC-R52-L4/ TC-R53-L4/	
Level 5	(12,61)	-	(26,61)		(31,61)	-	(41,61)
	TC-R11-L5/ TC-R13-L5		TC-R31-L5/ TC-R32-L5/ TC-R33-L5		TC-R41-L5/ TC-R43-L5/		TC-R61-L5/TC-R62-L5/ TC-R63-L5
Level 6	(12,63)	-	(26,63)	(28,63)	-	-	(41,63)
	TC-R11-L6/ TC-R12-L6		TC-R31-L6/ TC-R33-L6	TC-R34-L6/ TC-R35-L6/ TC-R36-L6			TC-R61-L6/TC-R62-L6/ TC-R63-L6

Installed (TC, PTs)	
Location	**Cell**
Injection line-vacuum part, TC-SBL-05	(3,40)
Injection line-pressurized part, TC-SBL-01, @ temperature BC	(50,19)
Injection line-pressurized part, PC-SBL-01, @ pressure BC	(50,19)
Injection line-vacuum part, PT-SBL-02	(3,40)
Expansion line, rupture disk, PT-S1B-04	(30,79)
Reaction vessel (S1B), PT-S1B-01/03	(50,56)
Reaction vessel (S1B), PC-S1B-01	(47,82)

Tab. 2: Location of the TCs and PTs in the SIMMER reference model

Time [ms]	Injected water [g]	T_{H2O} [°C]	$D_{orifice}$ [mm]	T_{PbLi} [°C]	T_{inj} [°C]	P_{inj} [bar]	P_{pipe} [bar]	P_{PbLi} [bar]	Description
0	50	295	0	327	340	161	19	2	Initial Value
42.5	-	-	4	-	-	148	-	-	Injector cap breakage
1145	-	-	4	-	307	109	-	-	Closing all valves
1300	-	-	4	-	307	126	-	-	stabilizing

Tab. 3: Post-test simulation matrix for Test D1.1 - Imposed Initial and Boundary conditions

3.2. Modified input deck for the sensitivity analysis

In addition to the reference case (i.e., Case #1), 4 new cases were developed to investigate the separate effects of the most relevant parameters (see Tab. 4):

Case #1: The reference case with the explained nodalization and models. This model was developed based on the acquired data from Test D1.1.

Case #2: The initial water volume fraction was set to 0.8 instead of 0.999 as in the reference case. This case represents the uncertainty effects due to preliminarily charged water into the injection line. All the other models and options were kept the same as the reference model.

Case #3: As explained in Test D1.1 procedure, the PbLi level is specified by means of measuring the melt temperature through the installed TCs at the top of perforated plate; therefore, the right level is in between and this issue changes the argon gas inventory in S1B. To evaluate the effect of the initial argon gas inventory, this case #3 was developed by adding 2 axial cells, representing 1 cm of increase in the argon gas volume length, from the top to PbLi region, and removing the same cells from the argon gas region. In fact, after this change, the PbLi region bounds between cells *J=45-71* and the argon region between *J=72-75*. All the other models and options were kept the same as the reference model #1.

Case #4: PbLi at 450°C was introduced as initial condition, this case presents the PbLi temperature effect on the PbLi/water interaction. All the other models and options were kept the same as the reference model.

Case #5: Water at 330°C was introduced as initial condition, this case presents the water temperature effect on PbLi/water interaction. All the other models and options were kept the same as the reference model.

Case#	m_{H2O} [g]	T_{H2O} [°C]	T_{PbLi} [°C]	P_{inj} [bar]	P_{pipe} [bar]	P_{PbLi} [bar]	V_{Ar} [m^3]	V_{PbLi} [m^3]	Description
1	**50**	**298**	**327**	**161**	**19**	**2.2**	**0.0035**	**0.02469**	**Reference case**
2	**40**	298	327	161	19	2.2	0.0035	0.02469	Volume fraction of water was set to 0.8 instead of 0.999
3	50	298	327	161	19	2.2	**0.0034**	**0.0247**	PbLi region includes the axial cells J=45-71, and cells J=72-75 for argon
4	50	298	**450**	161	19	2.2	0.0035	0.02469	PbLi at 450°C
5	50	**330**	327	161	19	2.2	0.0035	0.02469	Injection of water at 330°C

Tab. 4: Sensitivity test matrix for Test D1.1

4. Results and discussion

The related time trends and the resulting sequence of events for the most relevant parameters of the reference calculation are plotted against the experimental data, from Fig. 4 to Fig. 10. The reference calculation transient, during the injection, can be divided into different phenomenological windows, briefly summarized as below:

Phase 1 *[from Start of Transient (SoT) to 42.5 ms]:* Water injection line pressurization. As soon as the valve VP-SBL-06 opens, water starts to flow and to pressurize the pipeline upstream the injection cap. The start of the transient (t = 0 s) is selected as the time of the valve opening (see Fig. 4). At the same time, the pressurized water starts to move up and mixes with argon gas. As previously explained, in Test D1.1, 50 g of water are introduced into the injection line and there is not a continuous flow passing through the measuring cell (3,40); therefore, there is not a direct way to understand the exact thermodynamic condition of water in the injection line and the only way is to rely on the acquired data from TC-SBL-05 and PT-SBL-02 (to identify single or two phase condition for the injecting water). According to these signals, it proves that during the injection line pressurization phase, water temperature keeps under the saturation temperature, which means

vapor is not produced during phase 1. The pressure trends during phase 1, proves that the code accurately predicts the pressurization phase, with a small overestimation of the first peak in the injection line, as shown in Fig. 4. It turned out that some parameters have a significant influence on both the first peak and pressurization rate, which can be listed as: concentrated pressure loss coefficients (representing the losses at pipe bending and valves), initial water and gas pressure and temperature, amount of water, applied boundary and the position for these BCs in the injection line. The impact of such parameters has been considered in the sensitivity analysis and will be presented in the following.

Phase 2 *[from 42.5 ms to 1,145.2 ms]*: water and gas mixture flashing into S1B and the vessel pressurization followed by PbLi/water reaction. This phase can be further divided into three sub-phases:

(2a): Coolant water flashing and first pressure peak. The water injection and flashing in the liquid metal inside the reaction vessel causes a sudden steep pressure peak. The peak is high but also volatile, and it reaches 21 bar at cell (50,56), while the relevant recorded values for PT-S1B-01/02/03 range between 136-209 bar. After this initial peak, the pressure decreases slightly for a very short period (about 0.05 s), which is immediately followed by the next arising peaks (see Fig. 4). The SIMMER calculation reports more peaks at the very beginning of the flashing phase, but these peaks disappear faster comparing to the experimental signal. The pressure of the injected water represents a similar spike in the pressure of the injection line, shortly after the cap break-up time and then decreases due to pressurization of the reaction vessel. The pressurization signal in the injection line is reproduced by the numerical model for PT-SBL-02. The first peak value at PT-SBL-02 in the experiment is 120 bar, while it reaches 111 bar in the reference calculation.

(2b): Pressurization due to water and gas injection and hydrogen generation, characterized by the water injection and hydrogen production. The temperature trends show the PbLi/Water interaction inside the S1B vessel, the influence of this interaction is measured and plotted against the same relevant experimental data at the Test Section, refers to Tab. 2: for translating the position of TCs into the corresponding cells, see Fig. 5 and Fig. 7. Almost all the hydrogen is produced in this sub-phase, by the chemical reaction between the liquid PbLi alloy and water in both vapor and liquid phases. Indeed, the chemical reaction occurs between lithium in the alloy form and water, refer Fig. 10. According to Fig. 8, it turned out that the reference calculation overestimates the PbLi temperature compared to the experimental values. This impact might be explained as the result of the mixture temperature measuring in TCs, which is missing in the calculation. The SIMMER code does not calculate the temperature in mixture form by itself and it only gives values for the identified independent phases and density components. In this phase, all the injected water is exhausted by the chemical reaction with PbLi. The Fig. 9 illustrates the mass flow rate of water, which takes the zero value at the end of this sub-phase.

Nevertheless, in general, the trends give a similar phenomenological notion as for Test D1.1, by stating that the interaction impact on temperature is higher and earlier in time along both radial and axial directions. In other words, it means that the cells closer to the injector cap take more influence from PbLi/Water interaction, while this impact becomes lower and delayed in time for the outer cells.

(2c): characterized by the continuous gas injection up to the pressure equilibrium. During this sub-phase, the temperature measured by TCs in the Test Section did not show any significant variation while, in the same time frame, the pressure measured by Pressure Transducers (PTs) in S1B show a very linear increase, inclining towards the final equilibrium pressure. In this sub-phase, the most dominating effect is the argon gas pressure at the boundary cell (50,19), see Fig. 4.

Phase 3 *[from 1,145.2 ms to End of Transient (EoT)]*: system pressure stabilization, from the valve closing signal to the EoT. This phase is characterized by the stabilization of the pressure and temperatures in the system, which is immediately started by shutting off all the valves. This is to isolate the S1B vessel and prevent from either extra argon gas injection or reverse flowing of the liquid PbLi into the injection line and defecting the fast actuation valves. During this phase, the isolating valve VP-SBL-07 is closed, and the parameters (i.e. pressure in S1B) are stabilized.

From a qualitative analysis of the transient, the SIMMER-III code reasonably predicts the pressure and temperature trends. The final pressures in S1B stabilize in the simulation at 87.4 bar and between 87.2 and 89.2 bar (@ PT-S1B-01/02/03) in the experiment. The average temperature value at the end of the transient estimated by the code is 330 °C in S1B, while the average recorded values by TCs at EoT are 340 °C at the Test Section. The maximum temperatures occurring during the transient are 546 °C (@ TC-R12-L6) in the experiment and 559 °C for the reference calculation at cell (12,54), which corresponds with the TCs placed in the second level of the first ring. The maximum temperature values at the relevant TCs position are taken as a demonstrating evidence for the chemical reaction. Indeed, in the reference calculation, the code properly but not perfectly captures the temperatures in S1B.

The hydrogen production through the chemical reaction is estimated by the code (see Fig. 10), using the default options for the reference case and the total value is reported equal to 4.1 g at the end of phase 3. Total hydrogen acquired by the experiment is estimated equal to 3.1 ± 0.2 g and the stochiometric calculations give 2.8 g and 5.6 g, based on the two parallel chemical reactions (one producing Li_2O as product and the other one producing LiOH). Considering these values, it turns out that the code is able to predict the hydrogen value in line with the experiment and in the range of the stochiometric calculations.

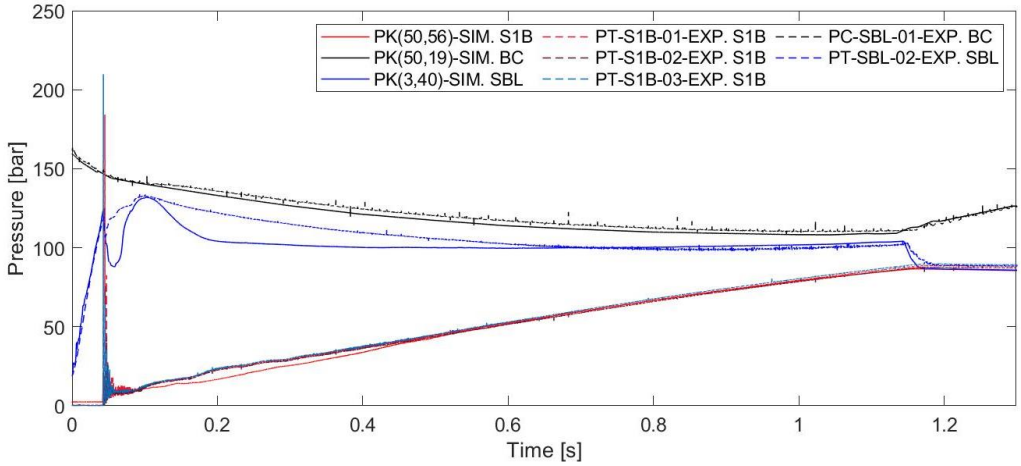

Fig. 4: Reference calculation: pressure (PK) compared with experimental data (PT) in S1B reaction vessel and in SBL injection line

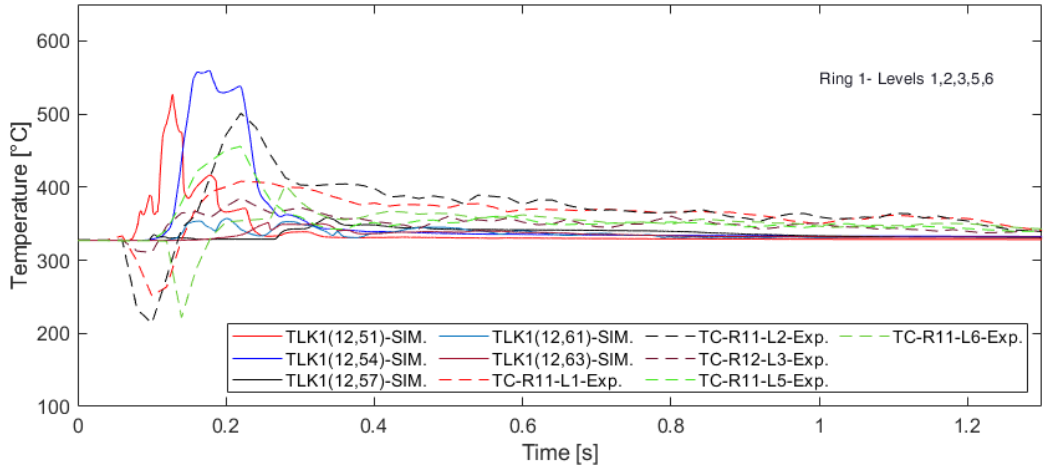

Fig. 5: Reference calculation: PbLi temperature (TLK1) compared with experimental signals (with the most relevant TCs), @Ring 1

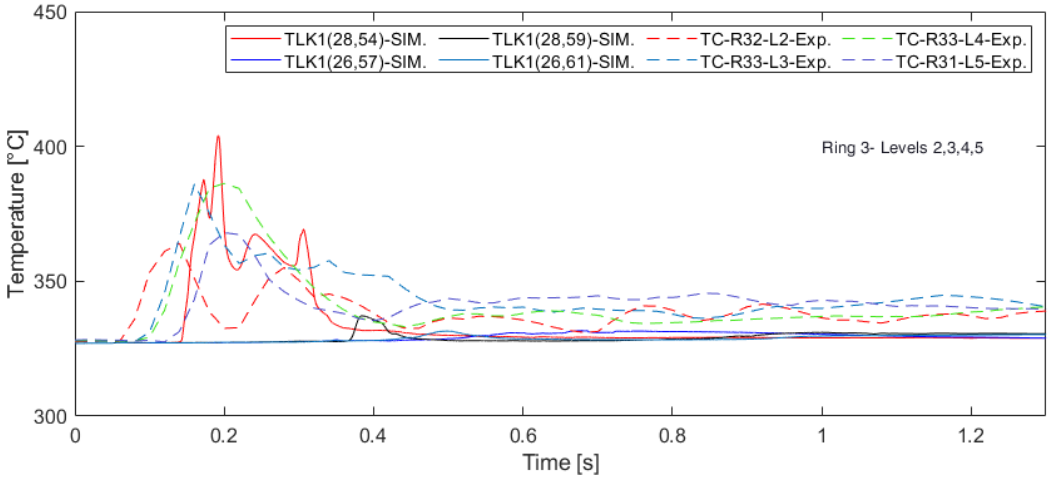

Fig. 6: Reference calculation: PbLi temperature (TLK1) compared with experimental signals (with the most relevant TCs), @Ring 3

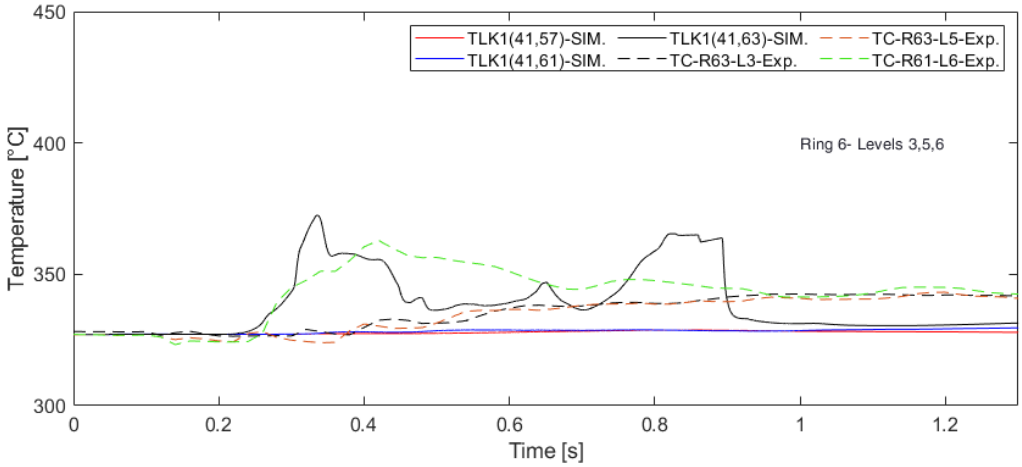

Fig. 7: Reference calculation: PbLi temperature (TLK1) compared with experimental signals (with the most relevant TCs), @Ring 6

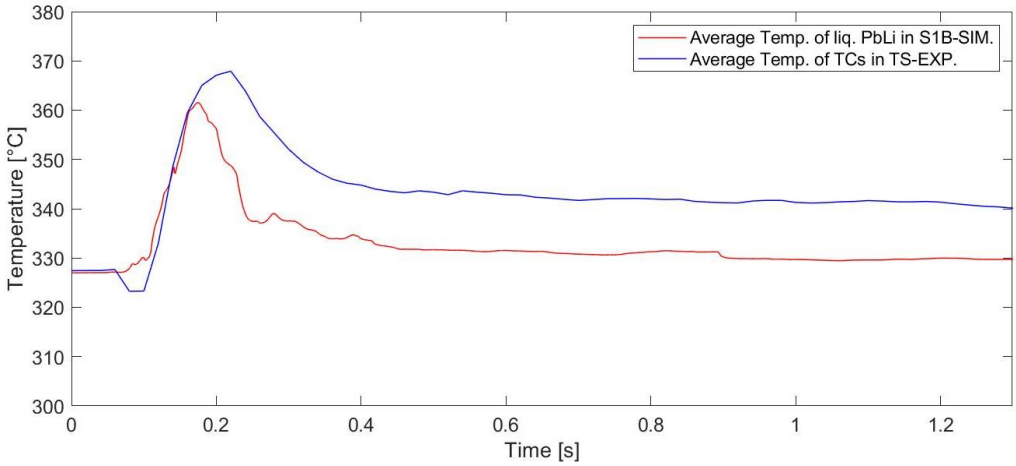

Fig. 8: Reference calculation: average temperatures of installed TCs in the Test Section

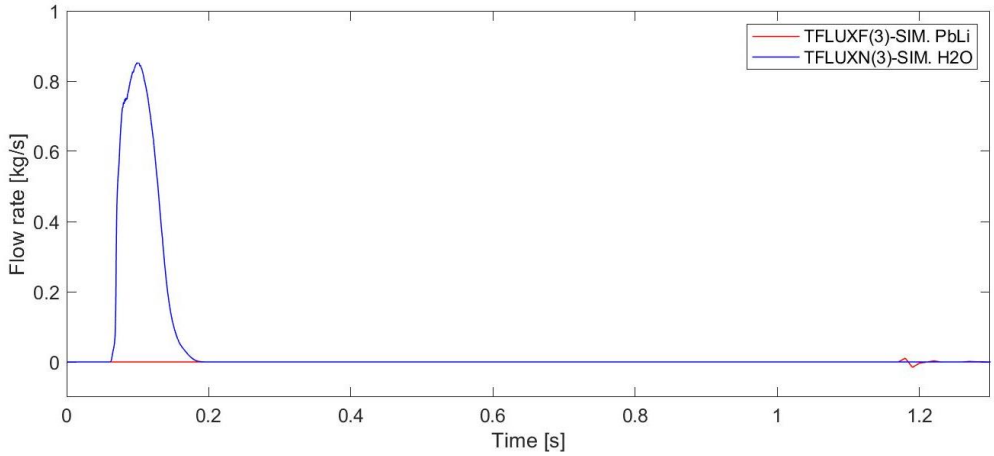

Fig. 9: Reference calculation: mass flow rate of PbLi (TFLUXF) and water (TFLUXN) at the injector cap

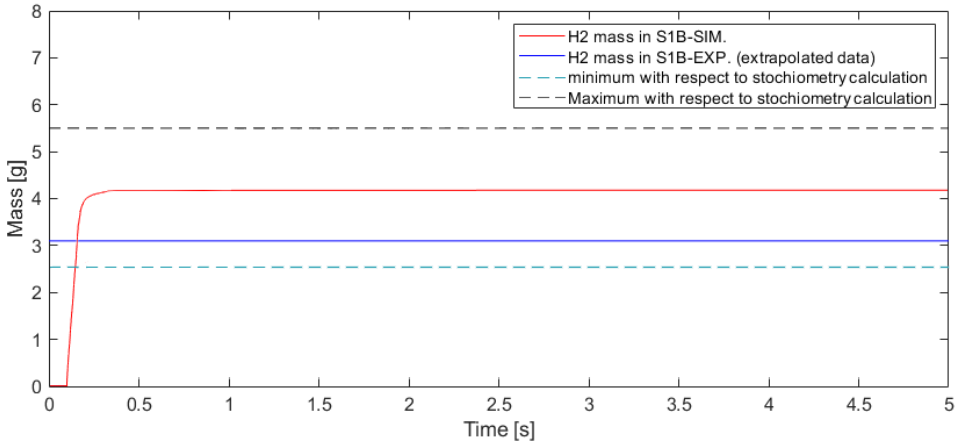

Fig. 10: Reference calculation: produced hydrogen by the chemical reaction

4.1. Qualitative analysis of code results

A comprehensive comparison between measured and calculated trends or values has been performed and analysed based on qualitative engineering judgments, including the following steps:

a) Qualitative analysis of code results and comparisons between experimental and calculated time trends, based on the selected variables (measurable parameters and phenomenological indicators);
b) Evaluation of the most relevant quantities for the assessment of phenomena/processes and for the safety, including the resulting sequence of the main events;
c) Evaluation of the accuracy based on selected figures of merit, identified and applied in refs. [20], [21].

The qualitative accuracy evaluation is based on identification of phenomenological windows and of the Relevant Thermal-hydraulic Aspect (RTA), (see Tab. 5 and Tab. 6) [22]. It essentially derives from a visual observation of the experimental and predicted trends. Then, the parameters characterizing the RTA (Single Value Parameter (SVP), Time Sequence of Events (TSE), Integral PArameter (IPA) and Non-Dimensional Parameter (NDP)) are quantified. These four group of parameters give information about the discrepancies between the experimental and the calculated results, which are qualified from Excellent to Unqualified. The determination of each figure of merit is explained in Tab. 7:.

#	EVENT DESCRIPTION	EXP. [ms]	CALC. [ms]	Note
1	Start of transient (VP-SBL-06 opening signal)	0	0	SOT
2	Vacuum line pressurization	0-42.5	0-42.5	Phase 1
3	Injector breaking-up	42.5	42.5	Start of Phase 2- first peak
4	Water flashing and first pressure peak	43.2	43.8	Phase 2 (a)
5	Ending of water injection	NA	185	Phase 2 (b)
6	Continuous argon injection	NA	185-1145.2	End of Phase 2 (c)-EoI
7	End of transient (VP-SBL-07 opening signal)	1145.2-5000	1145.2-5000	End of Phase 3-EoT

Tab. 5: Resulting sequence of main events for the reference calculation

RTA: REACTION VESSEL BEHAVIOR		UNIT	EXP	CALC	JUDG
TSE	Time of first pressure peak due to water flashing in S1B	ms	43	43.5	E
	Time of 10% total injected water	ms	NA	70.	-
	Time of 50% total mass flow rate	ms	NA	85.	-
	Time of 80% total mass flow rate	ms	NA	100	-
	Time of 100% total mass flow rate	ms	NA	700	-
SVP	S1B pressure at PT-S1B-01/02/03 @ first peak	bar	136.5-209.7	21	M
	S1B pressure at PT-S1B-01/02/03 @ EoPh2	bar	86.9-88.8	87.7	E
	S1B pressure at PT-S1B-01/02/03 @ EoPh3	bar	87.2-89.2	87.4	E
	S1B pressure at PT-S1B-04 @ first peak	bar	59.1	28.9	M
	S1B pressure at PT-S1B-04 @ EoPh2	bar	85.9	86.9	E
	S1B pressure at PT-S1B-04 @ EoPh3	bar	85.8	86.7	E
	S1B Abs. pressure at PC-S1B-01 @ first peak	bar	110.5	33.2	M
	S1B Abs. pressure at PC-S1B-01 @ EoPh2	bar	71.9	86.6	R
	S1B Abs. pressure at PC-S1B-01 @ EoPh3	bar	70.5	86.3	M
IPA	Integral mass of water @ EoPh1	g	0	0.0	E
	Integral mass of water @ EoPh2	g	NA	0.0	-
	Integral mass of water @ EoPh3	g	NA	0.0	-
NDP	Volume fraction of water @ injector break-up	--	NA	0.0	-
RTA: CHEMICAL REACTION INTERACTION					
TSE	Time of onset of H_2 production	ms	NA	71	-
	Time of end of H_2 linear generation	ms	NA	140	-
	Time of maximum PbLi temperature in S1B	ms	160	175	E
SVP	Max PbLi temperature in S1B	°C	547	559	R
	Min PbLi temperature in S1B	°C	195	324	-
	PbLi average temperature in S1B @ EoPh1	°C	327	327	E
	PbLi average temperature in S1B @ EoPh2	°C	341	330	R
	PbLi average temperature in S1B @ EoPh3	°C	340	330	R
	PbLi mass inventory in S1B @ EoT	kg	NA	192	-
	Mass of subcooled water in system S1B @ EoT	g	NA	0.0	-
	Mass of water vapor in system @ EoT	mg	NA	17	-
	H_2 linear generation rate @ EoPh2	g/s	NA	44.6	-
IPA	Integral H_2 production @ first pressure peak	g	NA	0.0	-
	Integral Hydrogen production @ EoPh1	g	NA	0.0	-
	Integral Hydrogen production @ EoPh2	g	NA	4.1	-
	Integral Hydrogen production @ 4.45 h	g	3.07	4.1	R
NDP	Volume fraction of water @ injector break-up	--	NA	0.99	-

Tab. 6: parameters characterizing the RTA for the reference calculation

#	Figure of merit	Symbol	Description
1	Excellent	E	calculation result lies within the uncertainty band of experimental data. The code predicts qualitatively and quantitatively the parameter
2	Reasonable	R	calculation result shows only correct behavior and trends. The code predicts qualitatively but not quantitatively the parameter
3	Minimal	M	calculation result lies within experimental data uncertainty band and sometimes does not have correct trends. The code does not predict the parameter, but the reason is understood and predictable
4	Unqualified	U	calculation result does not show correct trend and behavior, reasons are unknown and unpredictable. The code does not predict the parameter and the reason is not understood

Tab. 7: Determination of figures of merit, ref. [18]

4.2. Quantitative analysis of code results

In the present paper, according to ref. [23], the quantitative accuracy evaluation is defined as a systematic analysis of the deviation of the predicted relevant variables (which are the plotted variables in this study) with respect to the corresponding measured values. Considering the test as the reference, in terms of its execution and the availability of the

experimental data, the quantitative accuracy evaluation involves the pressures and temperatures in reaction and injection line.

Statistic approach

This approach is based on the time-averaging deviations of selected statistical parameters. The starting point is the definition of the DEV1 deviations Eq. (1), which is simply defined as the difference between calculated and experimental values, for each location at each time. Once the DEV1 deviations have been calculated, they can be "integrated" over the time interval (signal acquisition frequency). This leads to the three deviations DEV2: the first one represents the accumulative error Eq. (2), and will come out with a positive value if the local difference has been over-predicted and vice versa; the second is just summing-up the absolute deviation and will always be non-negative, Eq. (3); the third is a root mean square deviation, which enhances the contribution due to the large deviations, Eq. (4).

$$DEV1(t) = CALC(t) - EXP(t) \quad (1)$$

$$DEV2\_SIGN = \frac{1}{t_{end}-t_0}\int_{t_0}^{t_{end}} DEV1(t)\, d_t \quad (2)$$

$$DEV2\_ABS = \frac{1}{t_{end}-t_0}\int_{t_0}^{t_{end}} |DEV1(t)|\, d_t \quad (3)$$

$$DEV2\_RMS = \sqrt{\frac{1}{t_{end}-t_0}\int_{t_0}^{t_{end}} [DEV1(t)]^2\, d_t} \quad (4)$$

The results obtained for Case #1 as the reference calculations are reported in Tab. 8.

FFTBM approach

Another methodology suitable to quantify the code accuracy is called Fast Fourier Transform Based Method (FFTBM) and was developed at the University of Pisa (Refs. [21] and [22]). In general, each physical parameter can be demonstrated either in time domain form as a function of time ($F(t)$) or in frequency domain form as a function of frequency ($\tilde{F}(f)$), which represents the magnitude of the parameter at each frequency f. These two functions can be used to interchangeably derive each other, by means of the Fourier Transform. The integral form of this transformation is given by Eq. (5) and Eq. (6).

$$\tilde{F}(f) = \int_{-\infty}^{+\infty} F(t) e^{2\pi i f t}\, d_t \quad (5)$$

$$\tilde{F}(t) = \int_{-\infty}^{+\infty} \tilde{F}(f) e^{-2\pi i f t}\, d_f \quad (6)$$

The discretized form of these equations can be written as below:

$$\tilde{F}_n = \sum_{k=0}^{N-1} F_k e^{2\pi i k n/N} \quad (7)$$

$$F_k = \frac{1}{N}\sum_{n=0}^{N-1} \tilde{F}_n\, e^{-2\pi i k n/N} \quad (8)$$

Where:

$$\begin{cases} N = total\ number\ of\ data,\ \tau = sampling\ interval \\ F_k \equiv F(t_k), \quad \tilde{F}_n = \frac{1}{\tau}\tilde{F}(f_n) \\ t_k \equiv k\tau, \quad k = 0, 1, 2, \ldots., N-1 \end{cases} \quad (9)$$

The Fourier transform can be applied as a statistical tool for signal processing purposes. The discretized form is called Fast Fourier transform (FFT), which is an algorithm that rapidly computes the discrete Fourier transform. To apply it, functions must be identified by a number of values that is a power with base equal to 2 and the "sampling theorem" must be fulfilled. The "sampling theorem" requires avoiding the distortion of sampled signals due to aliasing occurrence [23]. The sampling theorem says: ''a signal that varies continuously with time is completely determined by its values at an infinite sequence of equally spaced times if the frequency of these sampling times is greater than twice the highest frequency component of the signal'' [24]. A full description about applying this method with all its' requirements, for quantitative code assessment purpose, is in ref. [25] but a summary of necessary variables and correlations are presented hereafter. The FFTBM shows the experimental–calculation discrepancies in the frequency domain form. For such a calculation, the experimental signal ($F_{exp}(t)$) and the calculational signal ($F_{Calc}(t)$) are needed to identify the error function as written in Eq. (10).

$$\Delta F(t) = F_{calc}(t) - F_{exp}(t) \quad (10)$$

The obtained error signal is used to calculate the amplitudes, together with the frequencies, and later for the Average Amplitude (AA) and Weighted Frequency (WF) that characterize the code's accuracy. For each variable, the AA (variable accuracy) is defined as the sum of the error function amplitudes normalized to the sum of the experimental signal amplitudes (see Eq. (11)). Furthermore, WF is defined as the sum of the frequencies multiplied (weighted) by the error function amplitudes, normalized to the sum of error function amplitudes, Eq. (12):

$$AA = \frac{\sum_{n=0}^{2^m} |\tilde{\Delta}F(f_n)|}{\sum_{n=0}^{2^m} |\tilde{F}_{exp}(f_n)|} \tag{11}$$

$$WF = \frac{\sum_{n=0}^{2^m} |\tilde{\Delta}F(f_n)| f_n}{\sum_{n=0}^{2^m} |\tilde{\Delta}F(f_n)|} \tag{12}$$

The most significant information is given by the factor AA, which represents the relative magnitude of the discrepancy deriving by the comparison between the addressed calculation and the corresponding experimental trend. The WF factor characterizes the kind of error because its value emphasizes whether the error has more relevance at low or high frequency ones. The higher is the weighted frequency, the more relevant is the contribution of the high frequencies to the average amplitude. The results of the FFTBM accuracy evaluation for the reference calculation are reported in Tab. 9.

The FFTBM has never been applied to these kind of interaction phenomena and thus this is rather a pioneering attempt to apply it. Nevertheless, it is expected to bring a further contribution to the SIMMER-III code validation, helping to identify most accurate code results, code models, and helping in the experimental test comprehension.

#	Parameter	Position	EXP-CALC	DEV2_SIGN	DEV2_ABS	DEV2_RMS
1	Pressure	Internal surface of S1B	PT-S1B-01/PK[50,56]	-2.1	2.3	5.0
			PT-S1B-02/PK[50,56]	-1.3	1.7	6.4
			PT-S1B-03/PK[50,56]	-2.7	2.9	6.8
			PT-S1B-04/PK[30,79]	0.5	2.3	4.9
			PC-S1B-01/PK[47,82]	-0.1	8.0	12.2
2	Pressure	SBL- below injector device	PT-SBL-02/PK[3,40]	-4.6	5.9	8.5
3	Temperature	Test section of S1B	TCs-R1-L1/TLK1[12,51]	-26.0	46.0	56.3
			TCs-R1-L2/TLK1[12,54]	-13.5	39.9	50.0
			TCs-R1-L3/TLK1[12,57]	-15.1	15.8	20.5
			TCs-R1-L5/TLK1[12,61]	-20.4	20.4	32.0
			TCs-R1-L6/TLK1[12,63]	-22.5	22.5	28.8
			TCs-R2-L2/TLK1[19,54]	-0.2	16.1	34.4
			TCs-R2-L4/TLK1[19,59]	-17.0	17.1	23.3
			TCs-R3-L1/ TLK1[26,51], [28,51]	0.8	7.4	14.6
			TCs-R3-L2/TLK1[28,54]	-1.6	9.2	13.7
			TCs-R3-L3/TLK1[26,57]	-13.3	13.3	18.3
			TCs-R3-L4/TLK1[28,59]	-13.0	13.1	17.4
			TCs-R3-L5/TLK1[26,61]	-16.0	16.0	22.2
			TCs-R3-L6/ TLK1[26,63], [28,63]	-10.7	10.8	12.1
			TCs-R4-L2/TLK1[31,54]	-1.1	4.5	2.4
			TCs-R4-L3/TLK1[31,57]	-9.5	9.5	11.5
			TCs-R4-L4/TLK1[31,59]	-13.7	13.7	19.7
			TCs-R4-L5/TLK1[31,61]	-13.3	13.4	16.3
			TCs-R5-L1/TLK1[35,51]	1.9	3.7	5.0
			TCs-R5-L4/TLK1[37,59]	-12.0	12.0	17.0
			TCs-R6-L3/TLK1[41,57]	-6.6	6.8	8.2
			TCs-R6-L5/TLK1[41,61]	-8.1	8.2	9.7
			TCs-R6-L6//TLK1[41,63]	-7.0	10.4	12.7
4	Temperature	SBL-below injector device	TC-SBL-05/TGK[3,40]	23.7	26.7	55.3

Tab. 8: Reference calculation: results of accuracy quantification for the selected parameters

#	Parameter	Position	EXP-CALC	F_cut [Hz]	Ph#	AA	WF
1	Pressure	Internal surface of S1B	PT-S1B-01 PK[50,56]	1/10/100	Ph1	4.48/4.48/4.12	0/0/1.1
					Ph2	0.05/0.05/0.09	0.44/2.0/30.72
					Ph3	0.04/0.05/0.09	0.41/2.06/30.64
					SoT-EoT	0.04/0.05/0.09	0.36/2.13/30.26
2	Pressure	Internal surface of S1B	PT-S1B-02 PK[50,56]	1/10/100	Ph1	12.04/12.04/8.21	0/0/1.2
					Ph2	0.04/0.05/0.08	0.57/2.12/29.12
					Ph3	0.04/0.05/0.08	0.54/2.18/29.02
					SoT-EoT	0.03/0.05/0.08	0.48/2.24/28.66
3	Pressure	Internal surface of S1B	PT-S1B-03 PK[50,56]	1/10/100	Ph1	16.55/16.55/10.92	0/0/2.09
					Ph2	0.05/0.06/0.09	0.36/2.13/27.21
					Ph3	0.05/0.06/0.09	0.33/2.21/27.11
					SoT-EoT	0.05/0.06/0.09	0.28/2.26/26.7
4	Pressure	SBL line	PT-SBL-02 PK[3,40]	1/10/100	Ph1	0.14/0.14/0.11	0/0/2.33
					Ph2	0.1/0.17/0.27	0.55/3.19/21.85
					Ph3	0.1/0.16/0.27	0.53/3.25/22.1
					SoT-EoT	0.1/0.15/0.26	0.49/3.3/22.53

Tab. 9: Reference calculation: summary of results obtained by the application of FFT-BM

4.3. Results for sensitivity analysis

As explained in the SIMMER model section, the selected sensitivities calculations are listed in Tab. 4, underlining the changed parameters, the relevant aspects, and the objectives, the full procedure of analysis is fully described in ref. [6]. The sensitivity calculation results are described and shown below, highlighting the differences that affect the adopted user choices, and differences and analogies with reference calculation Case#1. Then, the quantitative evaluation of the accuracy by the application of the FFTBM and of the statistics deviations, are illustrated. The pressure evolution and the average temperature of the liquid phase in S1B for all the sensitivity cases are shown from Fig. 11 to Fig. 13. According to Fig. 13, it turns out that in the sensitivity cases, amplitude of the average temperature peak is lowered due to the chemical reaction rate reduction. It also figured out that changing the initial temperatures of Water and PbLi do not significantly contribute to the chemical reaction magnitude, at least for low values of the water injection.

The evaluation of the accuracy is also performed for all sensitivity cases by comparing the calculated data with experimental results (calc-exp) up to EoT. All the results are depicted from Fig. 14 to Fig. 18. According to Fig. 14, the maximum and minimum DEV_sign from the experimental signal are connected to the Case #4 (in S1B) and the Case #3 (in SBL), which represent the cases with the higher initial mass and temperature for the PbLi, respectively. In addition, the highest values of DEV_abs also correspond to the Case #4 for both S1B and SBL. In Case #03 with more initial PbLi, the DEV_rms takes the highest value in SBL while the Case #04 with higher initial PbLi temperature is connected to the highest value for S1B. According to Fig. 17 and Fig. 18, the AA and WF parameters take the highest value in Case #1 as the reference case for both the S1B and SBL, which the values remain below 0.3 for AA and 27 Hz for WF.

The sensitivity cases pointed out the relevance of the initial and boundary conditions on the predictive capabilities of SIMMER-III code to simulate phenomena connected with lithium-lead/water interaction.

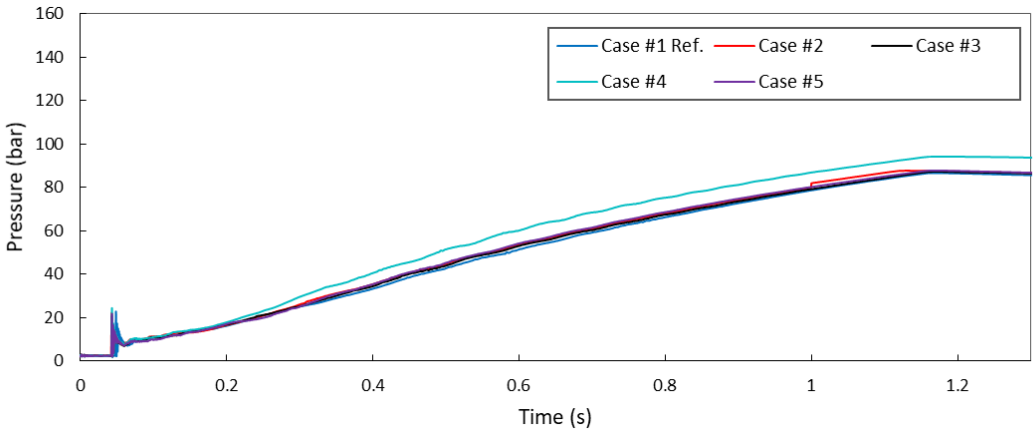

Fig. 11: Time trend of the pressure in S1B reaction vessel, reference calculation versus all sensitivity cases

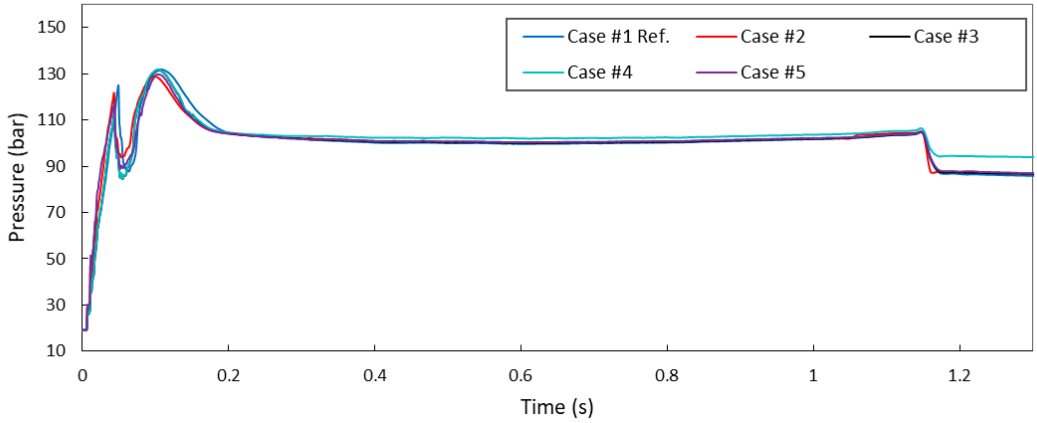

Fig. 12: Time trend of the pressure in SBL injection line, reference calculation versus all sensitivity cases

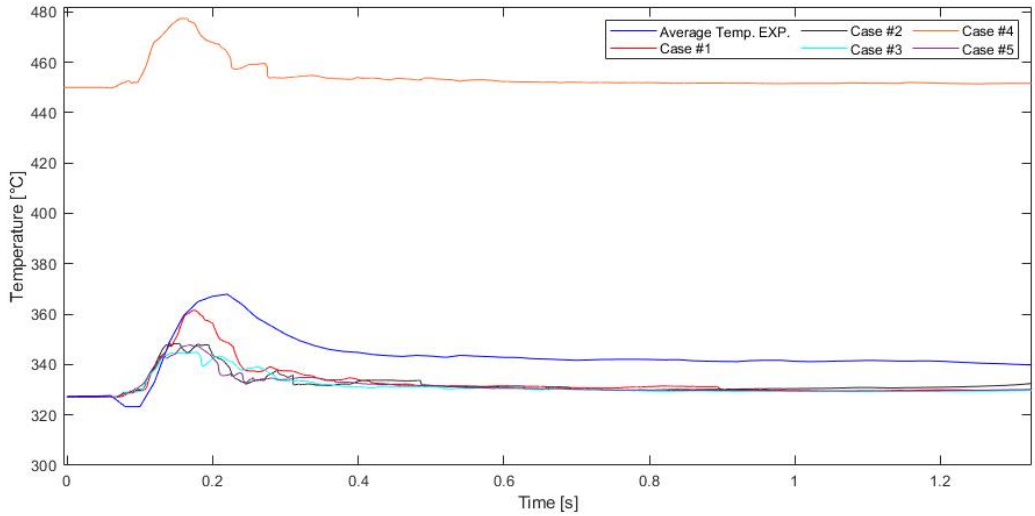

Fig. 13: Time trend of the PbLi average temperature in S1B, reference calculation versus all sensitivity cases

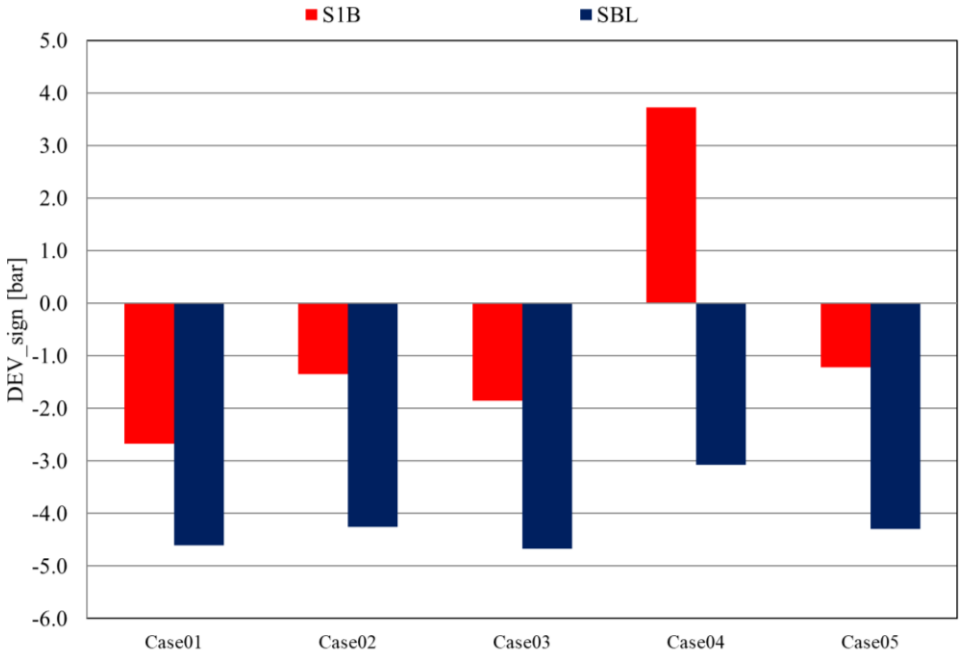

Fig. 14: Values for the selected figures of merit: DEV2_SIGN for PTs in S1B and SBL

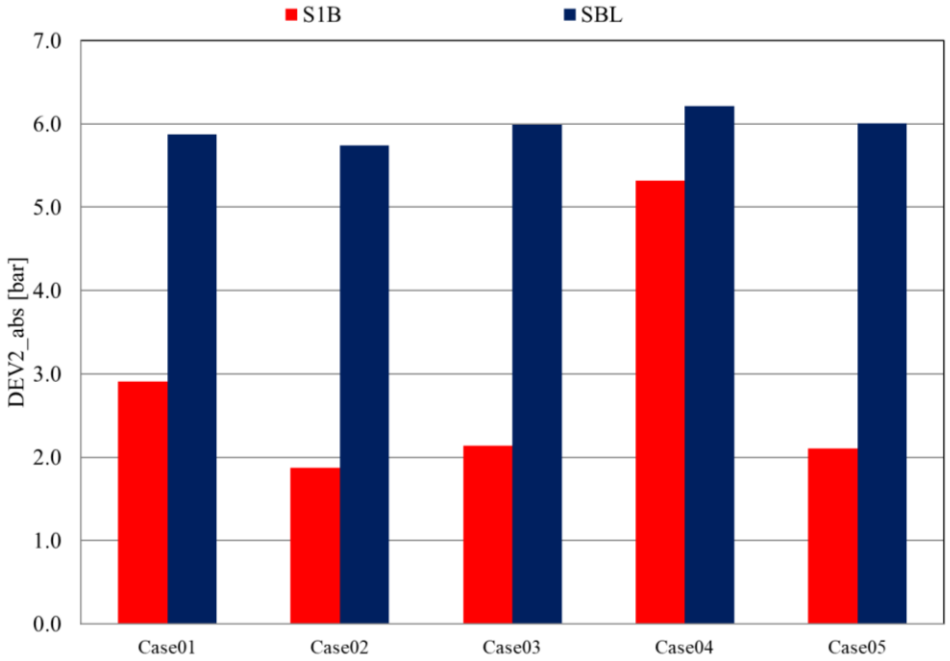

Fig. 15: Values for the selected figures of merit: DEV2_ABS for PTs in S1B and SBL

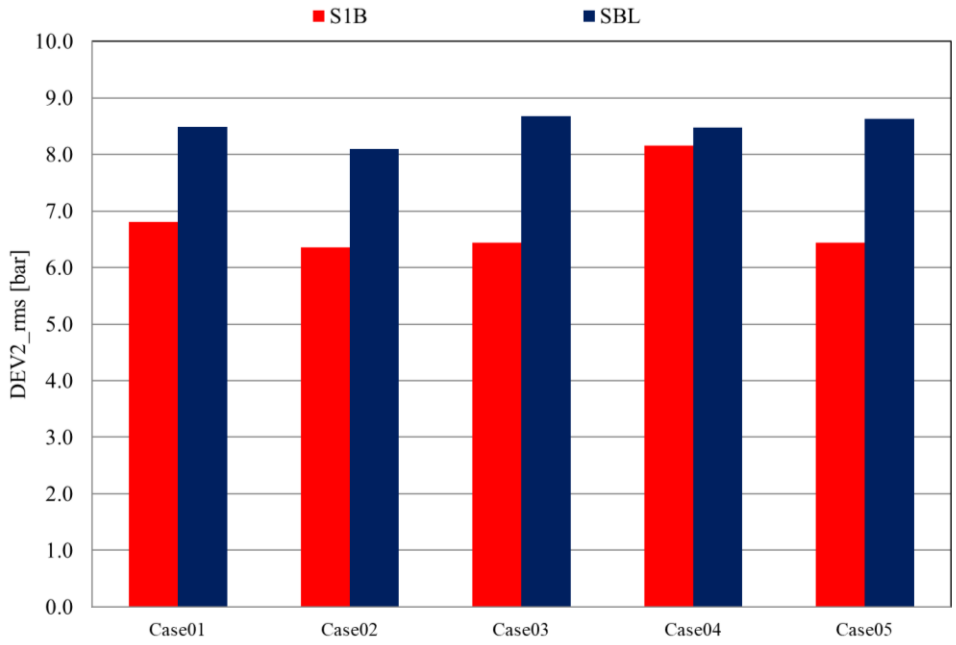

Fig. 16: Values for the selected figures of merit: DEV2_RMS for PTs in S1B and SBL

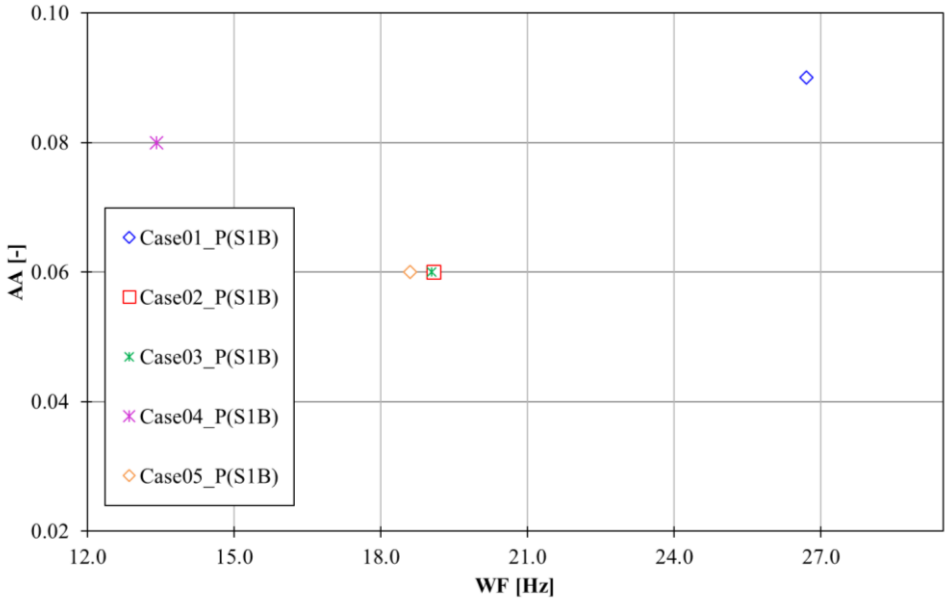

Fig. 17: Values of AA function of WF (FFTBM) evaluated at frequency cut of 100 Hz for reaction vessel pressure (S1B)

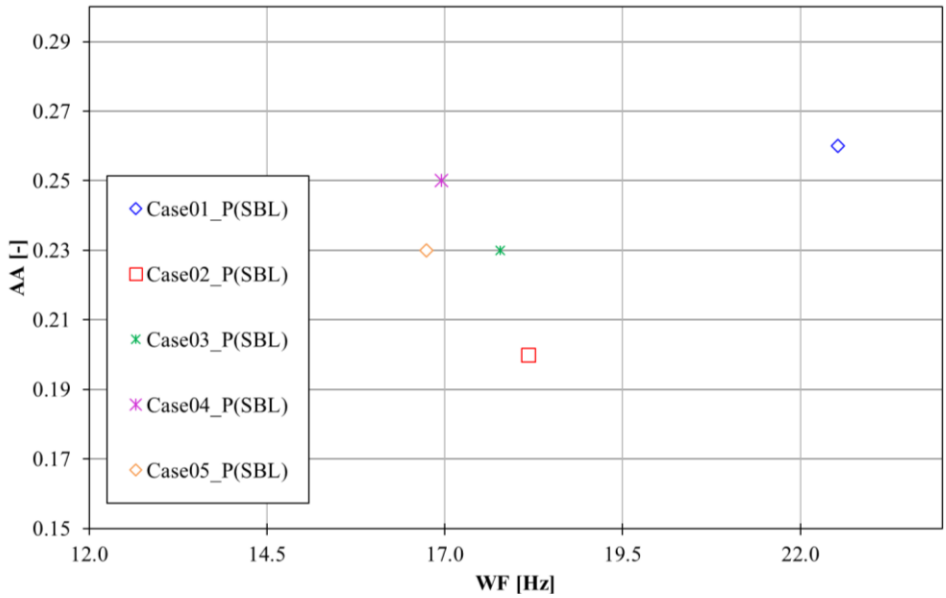

Fig. 18: Values of AA function of WF (FFTBM) evaluated at cut frequency of 100 Hz for injection line pressure (SBL)

5. Conclusion

This paper presents the validation of the SIMMER-III Ver.3F Mod.0.1 code, developed for fusion application at the University of Pisa, against the LIFUS5/Mod3 Series D experimental campaign. In particular, the work consisted in the simulation of the Test D1.1, with a series of sensitivity analyses focused mainly on improving the understanding of the experimental data. The specific outcomes from the reference post-test calculation of the LIFUS5/Mod3 Test D1.1 are outlined below:

- The SIMMER-III code predicts quite well the pressure of the injection line during all identified phases. The pressure trend is qualitatively in line with the experimental results, even though the rate of increase of the pressure in the injection line is slightly under-estimated;
- According to quantitative analysis results, the pressures calculated by the code perfectly align with the experimental signals both for the injection line and in S1B vessel and the order of deviations remains below the acceptable criteria;
- It turned out that SIMMER-III reasonably estimates the experimental results. The code correctly predicts the zones and the times in which the temperature starts to increase or decrease in S1B. However, the temperature values are mostly underestimated in S1B and overestimated in few spots, closer to the top vessel parts. The discrepancies can be explained by the fact that fragmentation and water-gas mixture distribution play an important role on specifying the interfacial area between the fluids and therefore the interaction/reaction itself;
- Based on a qualitative analysis, it turned out that the implemented chemical model acceptably predicts the hydrogen production during the transient by the chemical interaction of Lithium (in the form of PbLi eutectic alloy) and Water.

According to the outcomes of sensitivity analyses, the parameters, which more affect the code results are connected with the knowledge of the test initial and boundary conditions (i.e. the amount of the injected water or the initial volume of the cover gas, the temperature of water and PbLi). Most of the sensitivity cases pointed out the relevance of the initial and boundary conditions on the predictive capabilities of SIMMER-III code to simulate phenomena connected with the lithium-lead/water interaction.

The most influencing parameters are reported, as the initial amount and temperature of PbLi, plus the initial amount of water, the chemical reaction itself under the influence of available reactants (water and PbLi) and temperature of liquid PbLi.

According to the outcomes from the quantitative evaluation of the accuracy (all forms of DEVs and FFTBM), the best results are achieved in Case #2 and Case #5 calculations for the pressure and the average temperature of PbLi in S1B. Furthermore, considering the type of test and experimental data, 100 Hz could be considered an acceptable value for the

cut frequency. In all the performed sensitivity analyses, the results of average amplitude for the pressure of the reaction vessel are significant, considering that the values are AA<0.3.

In the future, the code validation phase will be followed by performing more post-test analyses on the updated available experimental data. Furthermore, the outcomes and achievements from this activity constitute an enhancement of the experience for conducting meaningful experiments for the TBM program simulations.

Acknowledgments

This work has been carried out within the framework of the EUROfusion Consortium and has received funding from the Euratom research and training programme 2014-2018 and 2019-2020 under grant agreement No 633053. The views and opinions expressed herein do not necessarily reflect those of the European Commission.

References

[1] L.V. Boccaccini, et al, Objectives and status of EUROfusion DEMO blanket studies, Fusion Eng. Des., 109–111 (2016), pp. 1199-1206.

[2] E. Martelli, et al, Advancements in DEMO WCLL breeding blanket design and integration, Int. J. of Energy Research, 42(1), 2018, pp. 27-52.

[3] A. Del Nevo, et al, WCLL breeding blanket design and integration for DEMO 2015: status and perspectives Fusion Eng. Des., 124 (2017), pp. 682-686.

[4] L.M. Giancarli, et al, ITER TBM Program and associated system engineering, Fusion Eng. Des. Vol. 136, Part B, 2018, pp. 815-821.

[5] S. Khani Moghanaki, A. Hedayat, Simulation and conceptual analyses of a stable natural core cooling system in an integrated small modular PWR, Nucl. Eng. Des. Vol. 332, 2018, pp. 357-373.

[6] S. Khani Moghanaki, et al, Validation of SIMMER-III code for in-box LOCA of WCLL BB: Pre-test numerical analysis of Test D1.1 in LIFUS/Mod3 facility, Fusion Eng. Des. Vol. 146, Part A, 2019, pp. 978-982.

[7] M. Eboli, et al, Experimental activities for in-box LOCA of WCLL BB in LIFUS5/Mod3 facility, Fusion Eng. Des., Vol. 146, Part A, 2019, pp. 914-919.

[8] B. Gonfiotti, et al, Development of a SIMMER/RELAP5 coupling tool, Fusion Eng. Des., Vol. 146, Part B, 2019, pp. 1993-1997.

[9] F. Galleni, et al, RELAP5/SIMMER-III code coupling development for PbLi-water interaction, Fusion Eng. Des., Vol. 153, 2020, 111504.

[10] M. Eboli, et al, Test Series D experimental results for SIMMER code validation of WCLL BB in-box LOCA in LIFUS5/Mod3 facility, 14th International Symposium on Fusion Nuclear Technologies, Budapest, 22-27 September 2019.

[11] F. Mascari, et al, Scaling issues for the experimental characterization of reactor coolant system in integral test facilities and role of system code as extrapolation tool, 16th International Topical Meeting on Nuclear Reactor Thermal Hydraulics (NURETH-16), Chicago, August 30-September 04, 2015.

[12] M. Eboli, Safety Investigation of In-Box LOCA for DEMO Reactor: Experiments and Analyses, PhD thesis, June (2017), https://etd.adm.unipi.it/theses/available/etd-05302017-093203.

[13] M. Eboli, N. Forgione, A. Del Nevo, Implementation of the chemical PbLi/water reaction in the SIMMER code, Fusion Eng. Des., 109-11 (2016), pp. 468-473.

[14] A. Pesetti, A. Del Nevo, N. Forgione, Experimental investigation and SIMMER-III code modelling of LBE–water interaction in LIFUS5/Mod2 facility, Nucl. Eng. Des., 290 (2015), pp. 119-126.

[15] A. Del Nevo, et al, Addressing the heavy liquid metal – Water interaction issue in LBE system, Prog. Nucl. Energy, 89 (2016), pp. 204-212.

[16] M. Eboli, et al, LIFUS5/MOD3 facility – Test D1.1 Experimental Data and Test Analysis Report, L5-T-R-400, July 2019.

[17] AA.VV., SIMMER-III (Version 3.F) Input Manual, O-arai Engineering Center, Japan Nuclear Cycle Development Institute, May 2012.

[18] S. Khani Moghanaki, et al, Report on post-test calculations with the SIMMER code vs LiPb-water experiments in the new LIFUS5/Mod3 facility WPBB-DEL-SAE-2.3.1-T01, Jan 2020.

[19] I.E. Idelchik, Handbook of Hydraulic Resistance, 3rd Edition, Jaico Publishing House, 2003.

[20] F. D'Auria, et al, Tsk 10 Final Report. Post-test analyses of GIDROPRESS mixing facility experiments, DIMNP NT 632 (08) Rev. 2, June 2008.

[21] W. Ambrosini, et al, Evaluation of accuracy of Thermal-hydraulic code calculations, J. Energia Nucl, Vol. 2, 1990.

[22] R.F. Kunz, et al, On the Automated Assessment of Nuclear Reactor Systems Code Accuracy, Nucl. Eng, Des., 211 (2002), pp. 245–272.

[23] A. Del Nevo, et al, Validation of advanced computer codes for VVER technology: LB-LOCA transient in PSB-VVER facility, Sci. Technol. Nucl. Installation, Vol. 2012, 480948, 15 pages.

[24] D. N. Lapendes, Dictionary of scientific and technical terms, 2nd ed. (1978), McGraw-Hill Book Company, New York, St. Louis, p. 1041.

[25] A. Prosek, F. D'Auria, B. Mavko, Review of quantitative accuracy assessments with Fast Fourier Transform Method (FFTBM), Nucl. Eng, Des., 217 (2002), pp. 179-206.

[26] F. D'Auria, et al, State of the Art in Using Best Estimate Calculation Tools in Nuclear Technology, Nuclear Engineering and Technology, Vol. 38, No. 1, Feb. 2006, pp 11-32.